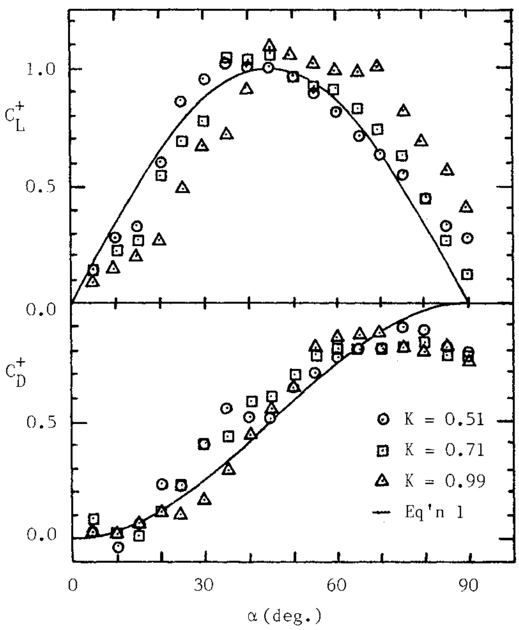

Fig. 4 Lift and drag correlations for high pitch rates.

Conclusions

Correlations for the lift and drag coefficients as a function of angle of attack and pitching rate have been obtained to a reasonable accuracy using simple trigonometric functions. Since all of the data were obtained at a single Reynolds number, using a NACA-0015 airfoil, and with an initial angle of attack equal to 0 deg, further expansion of the data base is needed.

Acknowledgment

This work was performed at the Sandia National Laboratories and was supported by the U.S. Department of Energy under Contract DE-AC04-76DP00789.

References

[1]Herbst, W., "Supermaneuverability," *Proceedings of Workshop on Unsteady Separated Flow,* U.S. Air Force Academy, Colorado Springs, CO, Aug. 1983, pp. 1–9.

[2]McCroskey, W. J. and Philippe, J. J., "Unsteady Viscous Flow on Oscillating Airfoils," *AIAA Journal,* Vol. 13, Jan. 1975, pp. 71–79.

[3]McAlister, K. W. and Carr, L. L., "Water Tunnel Visualizations of Dynamic Stall," *Journal of Fluids Engineering,* Vol. 101, Sept. 1978, pp. 376–380.

[4]Robinson, M. C. and Luttges, M. W., "Unsteady Flow Separation and Attachment Induced by Pitching Airfoils," AIAA Paper 83-0131, Jan. 1983.

[5]Martin, J. M., Empey, R. W., and McCroskey, W. J., "An Experimental Analysis of Dynamic Stall on an Oscillating Airfoil," *Journal of the American Helicopter Society,* Vol. 19, Jan. 1973, pp. 26–32.

[6]Harper, P. W. and Flanigan, R. E., "The Effect of Rate Change of Angle of Attack on the Maximum Lift of a Small Model," NACA TN2061, 1950.

[7]Ham, N. D. and Young, M. I., "Torsional Oscillations of Helicopter Blades Due to Stall," *Journal of Aircraft,* Vol. 3, May–June 1966, pp. 218–224.

[8]Francis, M. S. and Keesee, J. E., "Airfoil Dynamic Stall Performance With Large-Amplitude Motions," *AIAA Journal,* Vol. 23, Nov. 1985, pp. 1653–1659.

[9]Deekens, A. C. and Kuebler, W. R., "A Smoke Tunnel Investigation of Dynamic Separation," *Aeronautics Digest,* USAF A-TR-79-1, Feb. 1979, pp. 2–16.

[10]Daley, D. C., "The Experimental Investigation of Dynamic Stall," Thesis, Air Force Institute of Technology, Wright-Patterson AFB, Ohio, Rept. AFIT/GAE/AA/820-6, 1983.

[11]Walker, J., Helin, H., and Strickland, J., "An Experimental Investigation of an Airfoil Undergoing Large Amplitude Pitching Motions," *AIAA Journal,* Vol. 23, Aug. 1985, pp. 1141–1142.

[12]Walker, J., Helin, H., and Chou, D., "Unsteady Surface Pressure Measurements on a Pitching Airfoil," AIAA Paper 85-0532, March 1985.

[13]Strickland, J. H. and Graham, G. M., "Dynamic Stall Inception Correlation for Airfoils Undergoing Constant Pitch Rate Motions," *AIAA Journal,* Vol. 24, April 1986, pp. 678–680.

[14]Scraub, F. A., Kline, S. J., Henry, J., Runstadler, P. W., and Littell, A., "Use of Hydrogen Bubbles for Quantitative Determination of Time Dependent Velocity Fields in Low-Speed Water Flows," *Journal of Basic Engineering,* Vol. 87, June 1965, pp. 429–552.

[15]Graham, G. M., "An Experimental Investigation of an Airfoil Pitching at Moderate to High Rates to Large Angles of Attack," Ph.D. Dissertation, Texas Tech Univ., Lubbock, 1985.

Trailing-Edge Separation/Stall Alleviation

M. J. Werle,* R. W. Paterson,† and W. M. Presz Jr.‡
United Technologies Research Center
East Hartford, Connecticut

Introduction

THE overall problem addressed in this Note is that of reducing form drag due to boundary-layer separation in trailing-edge regions. As a representative application, attention is focused on airfoils at high lift conditions where, in general, loading capabilities are limited due to the occurrence of suction-surface boundary-layer separation. In such situations, the boundary layer is required to negotiate a strong adverse pressure rise as it approaches the trailing-edge region, resulting in boundary-layer separation (flow reversal). This boundary-layer separation results in a dramatic loss of lift and a drag increase as the airfoil begins to enter a stalled state.

The presence of such high lift separation/stall is difficult to predict, thus causing significant uncertainty for the design community. The consequence of overdesign is inefficient aerodynamics, whereas the cost of underdesign can be literally catastrophic. To date, nearly all mechanisms employed for overcoming these separation phenomena have been one of two types. The boundary layer has been energized either through the use of secondary air injection (slots, slats, blowing, etc.) or through the use of axial vortex generators (fins, troughs, grooves, etc.). Such devices achieve separation delay by energizing the boundary layer to overcome the adverse pressure gradients. The alternative approach described here focuses on providing a three-dimensional relief mechanism that permits the boundary layer to avoid the separation pressure rise. Presented herein is a brief description of the technical approach employed to develop this concept and initial results providing verification of the concept.

Technical Approach

The overall concept applied provides three-dimensional relief for a viscous boundary layer as it approaches a region of two-dimensional boundary-layer separation. This is accomplished by locally contouring the airfoil surface in the lateral direction, thereby establishing less unfavorable

Received Aug. 15, 1986.

*Manager of Gas Dynamics and Thermophysics. Associate Fellow AIAA.

†Manager, Experimental Gas Dynamics. Associate Fellow AIAA.

‡Consultant and Professor, Mechanical Engineering, Western New England College, Springfield, MA. Member AIAA.

pressure gradients than the axial adverse pressure gradients encountered by the two-dimensional boundary layer. Related surface contouring and/or distortion concepts employed previously (e.g., Refs. 1–3) focused mainly on the use of some form of axial vortex generators to energize the low-momentum fluid in the surface boundary layer. Here, the approach is to provide the local boundary layer an alternate path around the severest portion of the adverse pressure gradient, thus avoiding the extremely rapid drop in performance associated with the separation/stalling process.

This alternate boundary-layer path is established here using the surface-rippling approach, depicted in Fig. 1. Lateral surface contouring (ripples) scaled to the size of the anticipated two-dimensional separation bubble are distributed in the trailing-edge region of an airfoil. On the suction surface the ridges and troughs are constructed to cause small but significant lateral pressure gradients that drive the low-momentum fluid of the boundary layer toward a clashing line located somewhere between the peak and trough of the surface contours. This, then, allows the healthy, strong invisicid fluid to flow over the surface and more nearly attain the inviscid potential flow distribution in a spanwise average sense. The net result is a three-dimensional scrubbing of the initial two-dimensional boundary layer into a three-dimensional incipient axial vortex located somewhere between the peak and valley of the ripples. This produces an attached, nearly potential, surface-pressure distribution (albeit spanwise periodic) that maintains a high level of lift with high turning.

Additionally, the contouring provides the opportunity to accelerate locally the suction-side trailing-edge-region boundary layer through careful scheduling of the trough area cross section. Local acceleration on the suction surface is achieved at the expense of added diffusion of the pressure side boundary layer which, because of its more favorable pressure-gradient history, remains attached to the trailing edge.

A model airfoil contour resulting from this approach is shown in Fig. 2. The airfoil chosen for demonstration of the concept was a NACA-21% thick symmetric airfoil with the trailing-edge ripples superimposed around its normal contour. This airfoil thickness (21%) was chosen to avoid leading-edge separation during this demonstration. For this case the ripple height was 10% of chord, the axial extent of the ripples 57% of chord, and the peak-to-peak spacing in the spanwise direction 21% of chord. Note also that the troughs on the suction surface were narrower than their counterparts on the pressure surface to allow local area contraction (therefore acceleration) in the suction-surface-trough-base region.

Both a conventional straight and a rippled trailing-edge airfoil were tested in the same manner using a wind-tunnel force-balance system. The airfoil chord was 7.62 cm (3 in.), the span 22.86 cm (9 in.), and the freestream Reynolds number (based on chord) was 1.1×10^5. As shown in Fig. 2, a serrated boundary-layer trip (see Ref. 4) was provided in the leading-edge region to guarantee the presence of turbulent flow over the airfoil. In all cases reported here, only a small influence in the forces measured with or without the trip was noted, thereby indicating the presence of natural transition to a turbulent boundary-layer state. End plates were provided to isolate the sidewall boundary layers and provide more nearly two-dimensional test conditions.

Results

The influence of the rippled trailing edge (RTE) on the lift-and-drag characteristics of the airfoil tested is shown in Figs. 3 and 4. The dependence of the section lift curve on the angle of attack is presented in Fig. 3 for both the basic straight two-dimensional airfoil and the rippled trailing edge configuration. Here the lift coefficient shown is the section lift coefficient, that is, it has been averaged over the entire planeform span of the airfoil.

The maximum lift coefficient for the unmodified airfoil is seen to be approximately 0.73. This value for a Reynolds

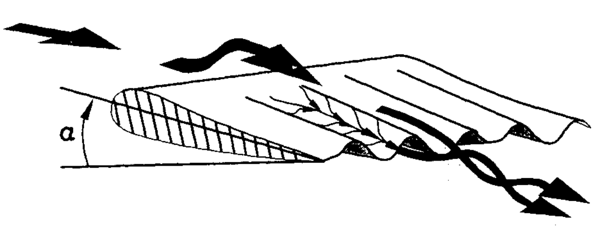

Fig. 1 The RTE concept (rippled trailing edge).

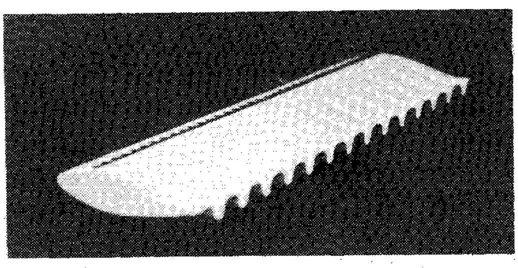

Fig. 2 RTE wind tunnel model.

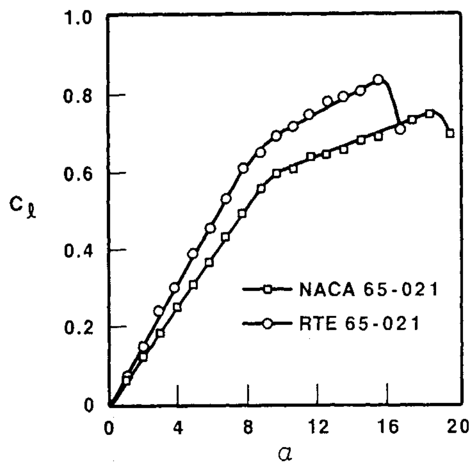

Fig. 3 RTE lift curve.

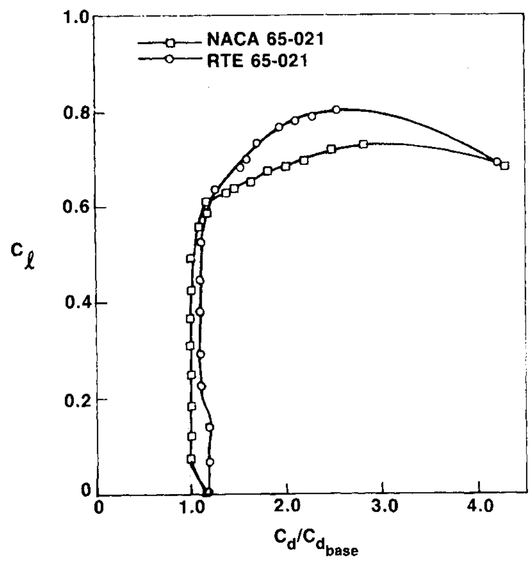

Fig. 4 RTE drag polar.

number of 1.1×10^5 is found to be consistent with a backward extrapolation of those data provided in Ref. 5 for Reynolds numbers varying from 3 to 9×10^6.

The marked increase in the lift coefficient with the addition of the rippled trailing edges is directly related to the alleviation of separation in the trailing-edge region at virtually all angles of attack. It is noted that the maximum lift coefficient is increased by approximately 12% (from 0.73 to 0.82) and occurs at an angle of attack 3 deg lower than that of the straight-trailing-edge case.

Drag polars for the two airfoils studied are presented in Fig. 4. These have been normalized with the minimum drag of the basic airfoil in order to isolate wind-tunnel installation effects and allow focus on the relative changes induced by the rippled trailing edge. Here it is seen that the basic airfoil displays a classical drag bucket with a rapid rise in the drag at a lift coefficient of approximately 0.6. The rippled trailing-edge airfoil shows a significantly wider drag bucket than its straight-trailing-edge counterpart. The relative increase in minimum drag for the RTE is expected due to the increase in wetted surface and three-dimensional skewing in the boundary layer. This latter effect is manifest in a spanwise periodic array of axial vortices emanating from the trailing edge as evidenced by complementary flow-visualization studies performed in a water tunnel with the same airfoil. The attendant drag increase for $C_L \leq 0.6$ is not considered of serious consequence because the principal focus here is increase of maximum lift through delay of the separation and stall process. In this regard, the RTE concept in Fig. 4 is seen to achieve this with a resulting significant increase in maximum lift/drag ratio.

Concluding Remarks

The results reported here clearly indicate that through use of controlled lateral-surface contouring, one can provide a mechanism for alleviation of boundary-layer separation effects and thereby produce aerodynamic shapes that yield higher maximum lift and/or lower drag at high lift. The basic separation/alleviation mechanism is the presence of local lateral pressure gradients that are less severe than the normal axial adverse pressure gradient that would otherwise exist in a trailing-edge region. These in turn provide a route for the low-momentum fluid in the surface boundary layer to be scrubbed off into clashing lines and high-momentum inviscid flow brought to the surface. This in turn permits the aerodynamic shape more nearly to achieve its potential flow equivalent lift while generating less drag than its separated-flow counterpart. Further study should now be conducted at high Reynolds numbers in more realistic high-lift situations.

Acknowledgments

This work was conducted as part of the UTRC independent research program. The authors wish to acknowledge the assistance of Mr. Paul Croteau, a former student at Western New England College, in conducting the experimental tests described here.

References

[1]Kimball, S., "Vortex Generators," *Road and Track*, Vol. 36, Jan. 1985, pp. 122–124.

[2]Schubauer, G. B. and Spangenberg, W. G., "Forced Mixing in Boundary Layers," *Journal of Fluid Mechanics*, Vol. 8, May 1960, pp. 10–32.

[3]Grose, R. M., "Theoretical and Experimental Investigations of Various Types of Vortex Generators," United Aircraft Corp., East Hartford, CT, Research Rept. R15362-5, 1954.

[4]Hama, F. R., "An Efficient Tripping Device," *Journal of the Aeronautical Sciences*, Vol. 24, March 1957, pp. 236–237.

[5]Abbott, I. H. and VonDoenhoff, A. E., "Theory of Wing Sections," Dover Publications, New York, 1959.

Pressure Fluctuation Measurements with Passive Shock/Boundary-Layer Control

S. Raghunathan*
The Queen's University of Belfast
Belfast, Northern Ireland

Nomenclature

C_p	= pressure coefficient
C	= model chord length
f	= frequency
H	= tunnel height
$\sqrt{nF(n)}$	= forcing function
M_{S0}	= shock Mach number at zero porosity
n	= frequency parameter fC/U_∞
ps	= porosity open area/model area
$\tilde{p}$	= rms pressure fluctuations
q_∞	= freestream freestream dynamic pressure
t	= thickness of model
U_∞	= freestream velocity
$x_{S0,T}$	= nondimensional shock position transducer position

Introduction

RECENT theoretical and experimental investigations[1-5] have demonstrated that a significant reduction in drag and increase in lift can be obtained in transonic flows with shock waves by the application of passive shock-wave/boundary-layer control (PSBL). The experiments of Theide et al.[4] seem to suggest that PSBL control can also suppress buffeting. However, there has been no attempt, to date, to measure in detail the unsteady aerodynamic excitation of pressure fluctuations in a passively controlled shock/boundary-layer interaction. This Note presents experimental results of pressure fluctuation measurements on a wall-mounted circular-arc half-model in a transonic tunnel with and without PSBL at shock Mach numbers 1.3 and 1.37.

Experiments

Experiments were performed in a blowdown transonic tunnel, 101 mm square with an atmospheric intake. The test section had closed sidewalls and roof, a slotted floor, and 9.6% porosity. The model was a circular-arc half-airfoil of 101-mm chord, 6% thickness, ratio, and 101-mm span, set on the tunnel roof, with the leading edge of the model 560 mm from the beginning of the constant-area test section (Fig. 1). Tunnel blockage $t/H = 6\%$, and effective chord-to-tunnel height $C/H = 0.5$. The recommended values are $t/H < 1.5\%$ and $C/H < 0.4$. However, these are not regarded as critical because the measurements were only of comparative nature. The momentum thickness Reynolds number at the foot of the shock $R = 10^4$. Although mounting a model on the tunnel roof in a small tunnel produced a relative boundary-layer thickness much larger than that encountered in free flight, the resulting momentum thickness Reynolds number at the foot of the shock of $R = 10^4$ was comparable to that which can be obtained by a model mounted in the freestream of larger tunnels. For the porous model, the porous region consisted of 1-mm-diam holes,

Received Dec. 18, 1985; revision received July 18, 1986.

*Senior Lecturer, Department of Aeronautical Engineering. Member AIAA.